AIChE Letter: Separations: Materials, Devices and Processes

Efficiency of Nitrogen Desorption from LiX Zeolite by Rapid Oxygen Purge in a Pancake Adsorber

Siew Wah Chai, Mayuresh V. Kothare and Shivaji Sircar
Dept. of Chemical Engineering, Lehigh University, Bethlehem, PA 18015

DOI 10.1002/aic.13983
Published online January 3, 2013 in Wiley Online Library (wileyonlinelibrary.com)

Significance

A nonequilibrium, nonisothermal, nonisobaric model was used for numerical simulation of the efficiency of N_2 desorption from a LiX zeolite column by rapid purge with O_2 in a pancake adsorber. The key parameters included desorption time, adsorbent particle size, and the adsorber length to diameter ratio. The efficiency was found to be a complex function of these variables.

Keywords: desorption of N_2, rapid O_2 purge, medical O_2 concentrator, pancake adsorber, LiX zeolite

Introduction

The conventional method of lowering the bed size factor (BSF, amount of adsorbent required to produce a specific flow rate of the product gas) of a pressure swing adsorption (PSA) process is to lower the total cycle time (t_c) in order to increase the cyclic frequency of the process. Several rapid PSA (RPSA) processes for production of 90+% O_2-enriched gas from a compressed air stream have been commercialized for use as a medical O_2 concentrator (MOC) where t_c is <10 s. LiX zeolite is the preferred N_2 selective adsorbent (after removal of H_2O and CO_2 from air) for this application [Henry's Law selectivity of adsorption of N_2 over O_2 is 7.53 at 298 K, and Henry's Law isosteric heats of adsorption of pure N_2 and O_2 are, respectively, 4.88 and 4.10 kcal/mol].

A recent publication by the present authors experimentally demonstrated that the BSF of a RPSA system for a MOC cannot be reduced indefinitely by reducing t_c due to impediments caused by finite ad(de)sorption mass-transfer rates, finite gas–solid heat-transfer coefficient, nonisothermal and nonisobaric (finite column pressure drop) operation. A mini adsorption column packed with ~350 μm particles of a commercial LiX zeolite and using a simulated Skarstrom-type RPSA cycle in conjunction with adsorption and desorption pressures of, respectively, 3 and 1 atmosphere was used in the test for MOC application. An optimum BSF of 40–50 (lbs/tons per day of contained O_2) with an O_2 recovery of ~25–30% from feed air, which were better performance than other published RPSA processes, could be obtained using a t_c of ~3–5 s.[1] Thus, the individual step times of an optimum RPSA process have to be fast lasting only 1–2 s.

We recently showed that the amount of product back purge used for desorption of N_2 from a zeolite column (a key step in design of a RPSA-MOC process) is a very sensitive variable in establishing both BSF and O_2 recovery, particularly for a rapid purge process.[2] A detailed numerical model was used to evaluate the effects of various mass-, heat-, and momentum-transfer resistances in a packed column on the purge gas quantity. The key findings were (a) ad(de)sorption mass-transfer resistance, nonisothermal column operation, and column pressure drop were major contributors to desorption inefficiency, (b) reducing adsorbent particle size increases adsorbate mass-transfer and gas–solid heat-transfer coefficients, but it also increases column pressure drop, resulting in an optimum particle size for a given desorption duty, and (c) a pancake adsorber [length (L)/diameter (D) < 1] may lower the negative effect of pressure drop, but hydrodynamic inefficiencies (maldistribution, particle agglomeration, etc.) may occur.[2,3]

The purpose of this note is to further report on the N_2 desorption efficiency by rapid O_2 purge in a pancake adsorber. The key conclusions derived from this simulation work provide some feasible considerations for operation of a pancake adsorber.

Mathematical Model for Simulation of N_2 Desorption by Rapid O_2 Purge

The model accounts for a finite adsorbate mass-transfer coefficient, a finite gas–solid heat-transfer resistance, axial

Correspondence concerning this article should be addressed to S. Sircar at sircar@aol.com.

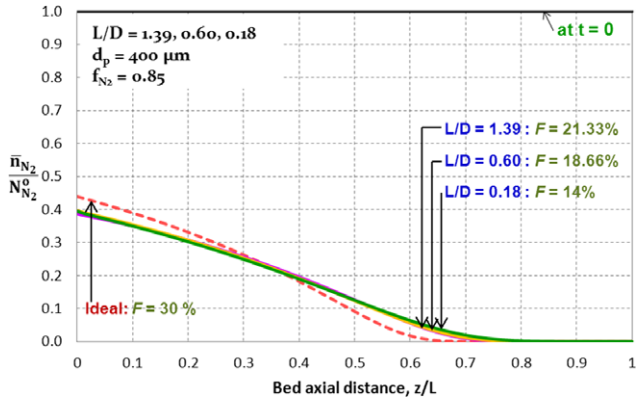

Figure 1. Simulated N_2 loading profiles in the column during desorption by O_2 purge.

[Color figure can be viewed in the online issue, which is available at wileyonlinelibrary.com.]

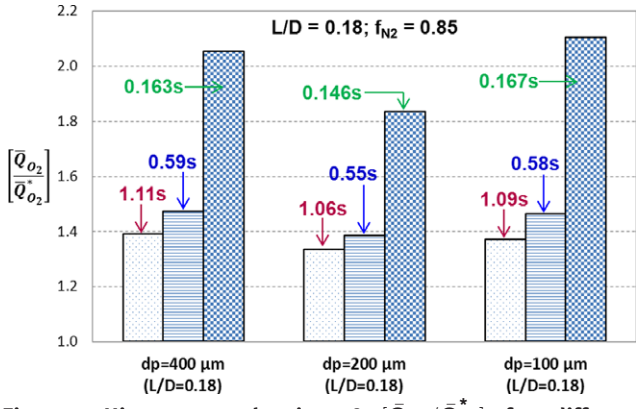

Figure 2. Histograms showing $\beta=[\bar{Q}_{O_2}/\bar{Q}^*_{O_2}]$ for different particle sizes and different purge durations (with varying mass flow rates) for pancake adsorber of L/D = 0.18.

[Color figure can be viewed in the online issue, which is available at wileyonlinelibrary.com.]

diffusion of mass and heat in the gas phase, and pressure drop in the column, along with a realistic boundary condition at the gas outlet end of the column for obtaining stable solutions of coupled partial differential equations describing the transfer processes.[4] Methods of numerical solutions can be found in Chai et al.[2]

Desorption of N_2 from an adiabatic LiX zeolite column saturated with a dry, CO_2-free synthetic air (21% O_2 + 79% N_2) at 298 K and 1 atm by rapid purging with pure O_2 entering the column under same conditions was considered. Rapid purge steps lasting for $\leq$1 s during which at least ~85% of total N_2 present in the column (adsorbed + void gas) removed from the column were simulated. The effects of various particle diameters (d_p = 100, 200, 300, 400, and 1500 μm) and column dimensions (L/D = 1.39 [conventional design] and L/D = 0.60, 0.18 [pancake design]) on N_2 desorption efficiency were evaluated. The total amount (W) of adsorbent (bulk density = 0.668 kg/L) in each case was constant (=0.16 kg). Thus, this study significantly extends the depth of our previously reported work that was limited to the evaluation of only a few cases (d_p = 200, 400, and 1500 μm; L/D = 1.39 and 0.18; and $t_{purge} \leq$ 2 and 10 s; Ref. 2).

Published correlations for relevant adsorptive properties and transport coefficients were used in the simulation. They included (a) adsorption equilibria for pure N_2, O_2, and their mixtures on LiX zeolite,[5] (b) linear driving force adsorbate mass-transfer coefficients for N_2 and O_2 on pelletized LiX zeolite crystals where the overall mass transfer is controlled by the pellet size due to binder macropore diffusion control,[6] (c) gas-phase mass axial dispersion coefficient,[7] (d) gas–solid heat-transfer coefficient in presence of gas thermal axial dispersion,[8] and (e) transient column pressure drop.[9] Specific values of these parameters can be found in Chai et al.[2]

Simulation Results

Typical results of the simulation exercise are shown in Figures 1–3. Figure 1 plots the local ratio of total N_2 loading (adsorbed + void gas) $[\bar{n}_{N_2}(z,t),$ mol/kg] to the total initial N_2 loading $[N^0_{N_2},$ mol/kg] at the start of the purge process (time t = 0), as a function of dimensionless column distance (z/L) for d_p = 400 μm, when 85% (f_{N_2}=0.85) of total N_2 initially present in the column was desorbed out of the column by O_2 purge (time t = t^*). The variable z (cm) is the distance in the column from the purge gas outlet end, and L (cm) is the total column length. Each simulation case was run for a given f_{N_2}, L/D, and d_p while varying purge time (t^*) and, hence, the purge gas mass flow rate.

Figure 1 shows N_2 loading profiles for different L/D ratios, when all transfer resistances listed earlier are included in the simulation. The values of t^* were, respectively, 1.21, 1.13, and 1.11 s for L/D values of 1.39, 0.6, and 0.18. The column inlet flow rate of O_2 purge gas (Q^o) used for each case was ~0.95 mol/(kg s), and the O_2 purge mass flow rates (mol/(m^2 s)) based on empty cross-sectional areas of the columns were, respectively, 53.5, 30.4, and 13.5 for L/D values of 1.39, 0.6, and 0.18. The total amount of O_2 purge gas used to achieve f_{N_2} = 0.85 is given by $\bar{Q}_{O_2}=[W \cdot Q^o \cdot t^*]$.

The dashed line in Figure 1 is the corresponding N_2 profile for the hypothetical, ideal case, where the purge operation is isothermal and isobaric, axial dispersion is absent,

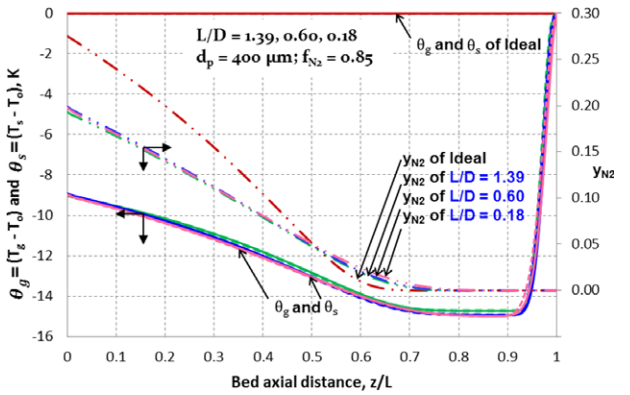

Figure 3. Profiles of gas and adsorbent temperatures and gas-phase N_2 mole fraction in adiabatic column undergoing N_2 desorption by O_2 purge.

[Color figure can be viewed in the online issue, which is available at wileyonlinelibrary.com.]

Table 1. Synopsis of Desorption Efficiency by Purge using Conventional and Pancake Adsorbers

Adsorber Length to Diameter Ratio (L/D)	O_2 Purge Gas Specific Flow Rate (Q^o, mol/(kg s))	O_2 Purge Gas Mass Flow Rate (mol/(m^2 s))	Desorption Time (t^*, s)	Relative Purge Quantity (β)	Percentage of N_2-Free Column Volume at End of Purge (F)
1.39	0.95	53.5	1.21	1.52	21.3
0.60	0.95	30.4	1.13	1.42	18.7
0.18	0.95	13.5	1.11	1.39	14.0
1.39	1.9	107	0.72	1.80	18.0
0.60	1.9	60.8	0.62	1.53	15.3
0.18	1.9	27.0	0.59	1.48	11.3
1.39	9.5	535	$\leq$0.2	Not able to achieve $f_{N_2} = 0.85$	
0.60	9.5	304	$\leq$0.2	Not able to achieve $f_{N_2} = 0.85$	
0.18	9.5	135	0.16	2.06	3.33

and the gas–solid adsorbate mass-transfer is instantaneous. The value of t^* was 0.8 s for the ideal case. The total amount of O_2 purge used in the ideal case is given by $Q^*_{O_2}$, which is the minimum amount of purge needed for a specific desorption duty. d_p or L/D have no effects on the ideal case desorption.

Figure 1 also shows the locations of the trailing edges of the desorption fronts (gas-phase N_2 mole fraction, $y_{N_2} < 0.0001$) at the end of the purge process when $f_{N_2} = 0.85$. Thus, Figure 1 gives the fraction (F) of the N_2-free adsorber volume at the end of a specific desorption duty. Consequently, F is an important quantitative measure of the efficiency of desorption by purge, and larger F is preferred for production of oxygen-enriched product gas by RPSA.[2]

Another useful parameter to quantify the efficiency of desorption by purge is the ratio $[\bar{Q}_{O_2}/\bar{Q}^*_{O_2}]=\beta$, which compares the amount of purge gas needed to that for the ideal case [$\beta = 1$] for a certain desorption duty (f_{N_2}). The variable β is > 1 in presence of any of the transport resistances listed earlier. Thus, lower the value of β, more efficient is desorption by purge. A systematic analysis of the effect of individual transport resistances on β was published by Chai et al.[2]

Figure 2 shows histograms of newly simulated values of β for a pancake adsorber ($L/D = 0.18$) packed with different sizes of sorbent particles and purged with different mass flow rates in accordance with the varying total purge durations. Given a total purge duration of 2 s at 13.5 mol/(m^2 s), the pancake absorber packed with 400, 200, and 100 μm adsorbent particle sizes could achieve a specific desorption duty of $f_{N_2} = 0.85$ at $t^* = 1.11$, 1.06, 1.09 s, respectively. Given a shorter total purge duration of 1 s at 27.0 mol/(m^2 s), the pancake absorber packed with 400, 200, and 100 μm adsorbent particle sizes, respectively, achieve $f_{N_2} = 0.85$ at $t^* = 0.59$, 0.55, and 0.58 s. Similarly, given a very short total purge duration of 0.2 s at 135 mol/(m^2 s), the pancake absorber packed with 400, 200, and 100 μm adsorbent requires $t^* = 0.163$, 0.146, and 0.167 s for achieving $f_{N_2} = 0.85$. These simulation results show that (a) β increases when the desorption time is decreased, and (b) there is an optimum d_p where β has a minimum for a given purge mass flow rate and t^*. These behaviors were observed for other values of L/D (0.60 and 1.39) used in our simulation in conjunction with various particle sizes and desorption times (not shown here). Another interesting result from this simulation was that a pancake adsorber ($L/D = 0.18$) could be used to obtain a high desorption duty of $f_{N_2} = 0.85$ while using a very fast desorption time of <0.2 s. That was not possible for adsorbers with larger L/D values (0.60 or 1.39).

Figure 3 shows the simulated profiles of gas-phase N_2 mole fraction (y_{N_2}), gas (T_g), and adsorbent (T_s) temperatures as functions of z/L in the column at the end of the purge process of Figure 1. T_0 is the initial column and the purge gas inlet temperature. The fairly complex column temperature–gas-phase composition profiles strongly influence the inefficiency during desorption by purge. These complex nuances are missed by the assumption of isothermal column behavior. Physical explanation of the thermal characteristics of an adiabatic desorption process described in Figure 3 can be found in Chai et al.[2] and Sircar and Kumar.[10] Two important observations are that (a) θ_g and θ_s have nearly identical profiles along the entire column length, and (b) y_{N_2} vs. z/L profiles are also apparently similar in the column irrespective of the L/D values. However, these small differences cause a substantial difference in the variable F as shown in Figure 1.

The variables β and F provide quantitative measures of efficiency of desorption by purge. Smaller β and larger F are preferred. Table 1 provides a synopsis of these variables for fast desorption [1.11 s $\leq t^* \leq$ 1.21 s], [0.59 s $\leq t^* \leq$ 0.72 s], and [$t^* \leq$ 0.2 s] of N_2 by O_2 purge from LiX zeolite particles ($d_p = 400$ μm) estimated by this work for $f_{N_2} = 0.85$ using different values of L/D.

Key conclusions from Figure 2 and Table 1 are that (a) a pancake adsorber ($L/D \leq 0.2$) may be needed to achieve high desorption duty $f_{N_2} \geq 0.85)$, when a small desorption time ($t^* \leq 0.2$ s) is used. However, that requires a very large purge gas quantity (β) while achieving a rather low N_2-free column volume (F) at the end of the purge step, thus, lowering the over-all desorption efficiency, (b) the effect of lowering L/D for a given t^* and d_p on the desorption efficiency is mixed (both β and F are reduced), (c) the desorption efficiency for a given f_{N_2} decreases (larger β and lower F) when t^* is reduced for a given L/D and d_p, and (d) the purge gas quantity (β) can be minimized for a given L/D and t^* by selection of an optimum d_p.

Literature Cited

1. Chai SW, Kothare MV, Sircar S. Rapid pressure swing adsorption for reduction of bed size factor of a medical oxygen concentrator. *Ind Eng Chem Res*. 2011;50:8703–8710.
2. Chai SW, Kothare MV, Sircar S. Numerical study of nitrogen desorption by rapid oxygen purge for a medical oxygen concentrator. *Adsorption*. 2012;18:87–102.

3. Zhong GM, Rankin PJ, Ackley MW. High frequency PSA process for gas separation. U.S. Patent 7,828,878 (2010).
4. Schiesser WE. PDE boundary conditions from minimum reduction of the PDE. *Appl Numer Math*. 1996;20:171–179.
5. Rege SU, Yang RT. Limits for air separation by adsorption with LiX zeolite. *Ind Eng Chem Res*. 1997;36:5358–5365.
6. Todd RS, Webley PA. Mass transfer models for rapid pressure swing adsorption simulation. *AIChE J*. 2006;52:3126–3145.
7. Ruthven DM. *Principles of adsorption and adsorption processes*. New York: Wiley, 1984.
8. Wakao N, Kaguei S, Funazkri T. Effect of fluid dispersion coefficients on particle-to-fluid heat transfer coefficients in packed beds. *Chem Eng Sci*. 1979;34: 325–336.
9. Ergun S. Fluid flow through packed columns. *Chem Eng Prog*. 1952;48:88–94.
10. Sircar S, Kumar R. Equilibrium theory for adiabatic desorption of bulk binary gas mixtures by purge. *Ind Eng Chem Process Des Dev*. 1985;24:358–364.

Manuscript received Jun. 18, 2012, and revision received Nov. 5, 2012.